A Mechanism for Abrupt Climate Change Associated with Tropical Pacific SSTs*

STEVE VAVRUS, MICHAEL NOTARO, AND ZHENGYU LIU

Center for Climatic Research, University of Wisconsin—Madison, Madison, Wisconsin

(Manuscript received 26 April 2004, in final form 16 March 2005)

ABSTRACT

The tropical Pacific's response to transiently increasing atmospheric CO_2 is investigated using three ensemble members from a numerically efficient, coupled atmosphere–ocean GCM. The model is forced with a 1% yr^{-1} increase in CO_2 for 110 yr, when the concentration reaches 3 times the modern concentration. The transient greenhouse forcing causes a regionally enhanced warming of the equatorial Pacific, particularly in the far west. This accentuated equatorial heating, which is slow to arise but emerges abruptly during the last half of the simulations, results from both atmospheric and oceanic processes. The key atmospheric mechanism is a rapid local increase in the super–greenhouse effect, whose emergence coincides with enhanced convection and greater high cloud amount once the SST exceeds an apparent threshold around 27°C. The primary oceanic feedback is greater Ekman heat convergence near the equator, due to an anomalous near-equatorial westerly wind stress created by increased rising (sinking) air to the east (west) of Indonesia. The potential dependence of these results on the specific model used is discussed.

The suddenness and far-ranging impact of the enhanced, near-equatorial warming during these simulations suggests a mechanism by which abrupt climate changes may be triggered within the Tropics. The extratropical atmospheric response in the Pacific resembles anomalies during present-day El Niño events, while the timing and rapidity of the midlatitude changes are similar to those in the Tropics. In particular, a strengthening of the Pacific jet stream and a spinup of the wintertime Aleutian low seem to be forced by the changes in the tropical Pacific, much as they are in the modern climate.

1. Introduction

The Tropics are known to be an important source of large-scale climate variability, primarily through ENSO, and thus may be expected to play an important role in affecting past and future global climate changes. By virtue of their vast extent and teleconnective forcing, the Tropics can cause a low-latitude heating anomaly to translate into one of global scale, such as the 1997/98 El Niño, which helped to generate the warmest global-mean temperature on record (Houghton et al. 2001). The importance of ENSO in the present climate has sparked many studies that have investigated how this mode of variability may change under future greenhouse warming (e.g., Meehl and Washington 1986; Knutson and Manabe 1995; Cai and Whetton 2000). While classical studies cite central and eastern Pacific SST anomalies as a means of driving variations in standing wave patterns such as the Pacific–North American (PNA; Horel and Wallace 1981), recent work indicates that remote tropical forcing of midlatitude circulation may be more widespread. These teleconnections include the North Atlantic Oscillation (NAO) forced by Indian and Pacific Ocean temperatures (Hoerling et al. 2001), as well as SST anomalies in the tropical oceans of the North Atlantic (Terray and Cassou 2002) and South Atlantic (Robertson et al. 2000). The Indo-Pacific warm pool region appears to be an especially effective location for driving remote changes, as evidenced by simulations of pronounced extratropical teleconnections in the Northern Hemisphere due to atmospheric heating by both SST anomalies and Indonesian deforestation (Branstator 1985; Chase et al. 2000; Neale and Slingo 2003).

In this paper we focus on the causes and importance of changes in the deep tropical Pacific under greenhouse forcing. We pay particular attention to the rapidity of the equatorial heating during the latter stages of

* Center for Climatic Research Publication Number 857.

Corresponding author address: Dr. Steve Vavrus, Center for Climatic Research, University of Wisconsin—Madison, 1225 W. Dayton Street, Madison, WI 53706.
E-mail: sjvavrus@wisc.edu

simulations forced with transient increases in CO_2. We use an updated version of the Fast Ocean–Atmosphere Model (FOAM), a low-resolution, coupled atmosphere–ocean GCM that has been used in previous studies of past and future climate changes (Liu et al. 2000; Wu et al. 2003; Poulsen 2003; Delire et al. 2001). We present the results from three ensemble simulations, all of which are driven by a 1% yr^{-1} CO_2 increase but started from slightly different initial conditions, to show the response of the tropical Pacific and the impact on the North Pacific due to greenhouse forcing. Additional supplemental ensemble simulations are used to test the sensitivity of the model to changes in oceanic wind stress forcing and to the increased tropical SSTs.

We describe the model and briefly depict its modern control simulation in section 2. This introduction is followed in section 3 by a description of the GCM's transient CO_2 simulations, consisting of a detailed analysis of the tropical Pacific response and the impact of the tropical warming on the extratropical Pacific atmosphere. We continue in section 4 with possible implications of this work for past and future climate changes, then follow with concluding remarks in section 5.

2. Model description

The model used in this study is the fully coupled, global, atmosphere–ocean model FOAM, version 1.5 (hereafter referred to as FOAM1.5), which was developed at the University of Wisconsin. This is an improved version of the original FOAM (version 1.0), which is described in detail in Jacob (1997) and has been used in a number of recent studies to investigate tropical climate variability and sensitivity (Liu et al. 2000; Harrison et al. 2003; Liu et al. 2003; Wu and Liu 2003; Notaro et al. 2005). The model consists of a low-resolution atmosphere (spectral R15 or approximately 4.5° latitude × 7.5° longitude) coupled to a 1.4° × 2.8° land surface and ocean grid. The atmospheric component is essentially a lower-resolution variant of National Center for Atmospheric Research (NCAR) Community Climate Model version 3.6 (CCM3.6; Kiehl et al. 1998), which is used in NCAR's Climate System Model (CSM1), and uses the same diagnostic cloud liquid water parameterization as in CSM1 (Boville and Gent 1998). The ocean component is similar to the Geophysical Fluid Dynamics Laboratory (GFDL) Modular Ocean Model (MOM) and uses 24 levels (20-m top ocean layer) and the thermodynamic sea ice code of the CSM1. FOAM1.5 uses improved snow albedo and sea ice parameterizations over version 1.0 and has higher vertical ocean resolution compared with the original 16-level FOAM. This GCM is highly efficient on parallel computing systems, is successful at capturing major climate features, and produces a stable long-term climate simulation without the use of flux adjustments (Wu et al. 2003).

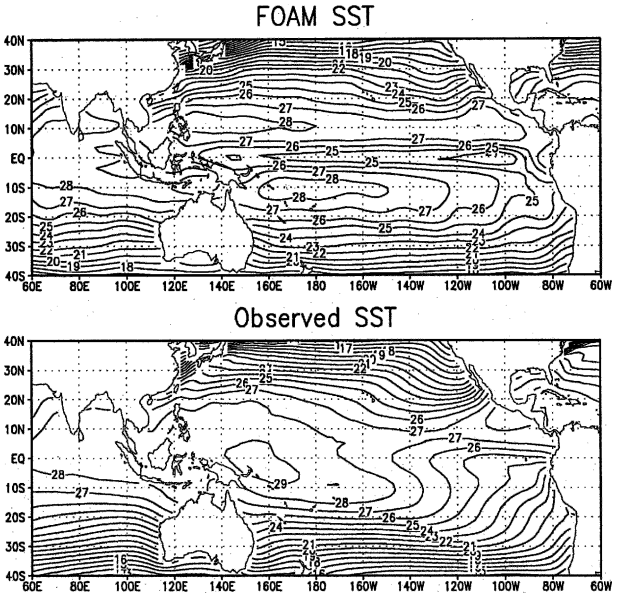

FIG. 1. Modern annual SSTs (°C) over the Indo-Pacific Oceans as (top) simulated by FOAM1.5 and (bottom) observed (Levitus 1982).

The modern control simulation of FOAM1.5 generates a global mean surface air temperature (286.7 K) similar to observations (287.0 K) from the National Centers for Environmental Prediction (NCEP)–NCAR reanalysis (Kalnay et al. 1996). The simulated tropical (30°S–30°N) temperature bias is −0.51 K, primarily due to the equatorial Pacific cold tongue extending too far westward, a common problem in climate models (Murtugudde et al. 2002) (Fig. 1). Although the cold tongue bias affects the location of the rapid tropical warming discussed below, the physical mechanisms responsible for this abrupt climate change should operate regardless of the associated displacement of the Indo-Pacific warm pool.

3. Results

a. Tropical Pacific response

The results of the greenhouse experiments were derived from three ensemble members, whose starting points were separated by 8 yr during the final century of a 1000-yr control integration using near-modern CO_2 concentration (335 ppmv). The gradual 1% yr^{-1} rise in CO_2 over the 110-yr integrations leads to a tripling of CO_2 by the end of the simulation (no other greenhouse gases or aerosols were changed). FOAM1.5's transient climate response (the global surface air temperature

rise at the time of CO_2 doubling) of 1.1 K is the same as that of the Community Climate System Model, version 2 (CCSM2), but is relatively low compared with the suite of models used in the Coupled Model Intercomparison Project (CMIP; Holland and Bitz 2003). The global mean warming by the end of the simulations is fairly similar and linear among the three ensemble members, ranging from 1.6 to 2.0 K, but the temperature displays interannual and decadal fluctuations due to internal variability in the climate system (Fig. 2). The primary focus of this paper is on the response of the tropical Pacific Ocean, whose eventual warming pattern near the end of the simulation shows a large spatial variability in the ensemble mean (Fig. 3) that is similar to the pattern in all three simulations (not shown). Over the low–midlatitude Pacific and Indian Oceans, the model produces the largest zonal SST increases in the near-equatorial Pacific, with the maximum warming of nearly 2 K just east of Indonesia. The greater heating in the deep Tropics relative to the subtropics is somewhat surprising, given the tendency for models to amplify the global warming signal in higher latitudes, but this pattern is reminiscent of the SST changes in several other transient greenhouse experiments (Liu et al. 2005).

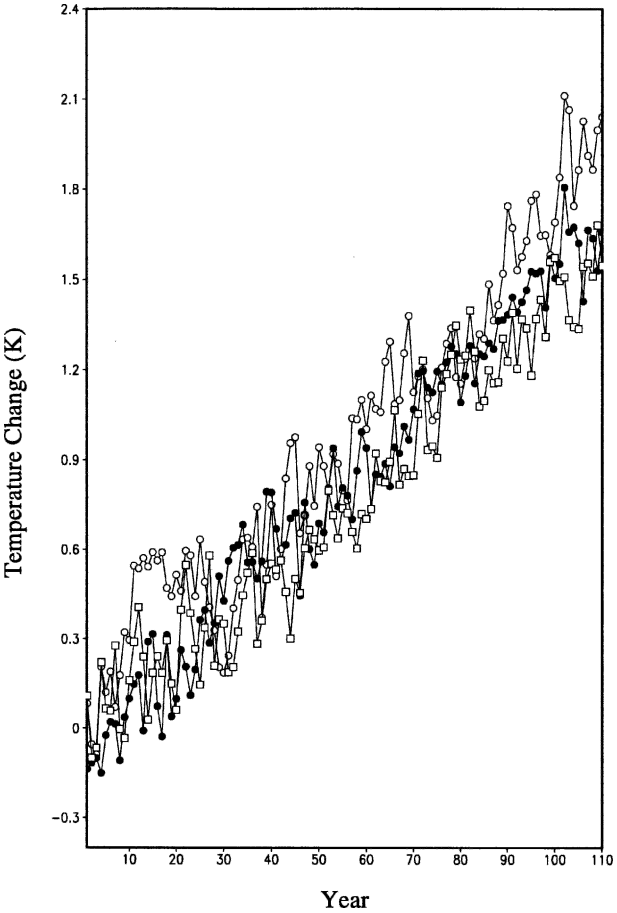

FIG. 2. Globally averaged surface air temperature anomaly (K) forced by a 1% yr^{-1} transient CO_2 increase for the three ensemble members. The members were initialized from conditions 8 yr apart near the end of the 1000-yr modern control simulation.

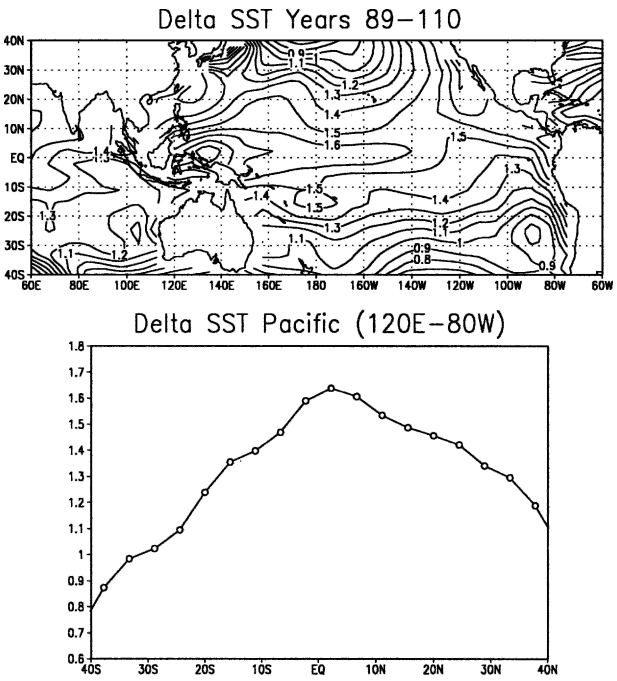

FIG. 3. (top) Change in ensemble-mean annual SST (K) during the final two decades of the transient CO_2 simulation, and (bottom) the zonally averaged change in SST over the Pacific Ocean (120°E–80°W).

The enhanced equatorial warming is highly correlated with the change in the outgoing longwave (LW) radiation flux at the top of the atmosphere (TOA), which becomes strongly negative during the simulation over the regions of maximum SST increase (Fig. 4). The decreased TOA infrared radiative emission is most strongly associated with the SST changes within the deep Tropics (20°S–20°N), where the spatial correlation coefficient between the two patterns is −0.5. The maximum negative LW is collocated with the maximum warming, both zonally averaged and especially in the western equatorial Pacific, where the negative LW anomaly peaks at -12 W m^{-2}. The decrease in TOA LW is caused by the absorption of surface longwave radiation in the upper troposphere and the reemission of longwave radiation to space at much lower temperatures than the SSTs. A negative TOA LW anomaly associated with an increase in SST is a definition of the super–greenhouse effect (SGE; Bony et al. 1997), which is a positive feedback occurring when greenhouse trapping of infrared radiation with increasing

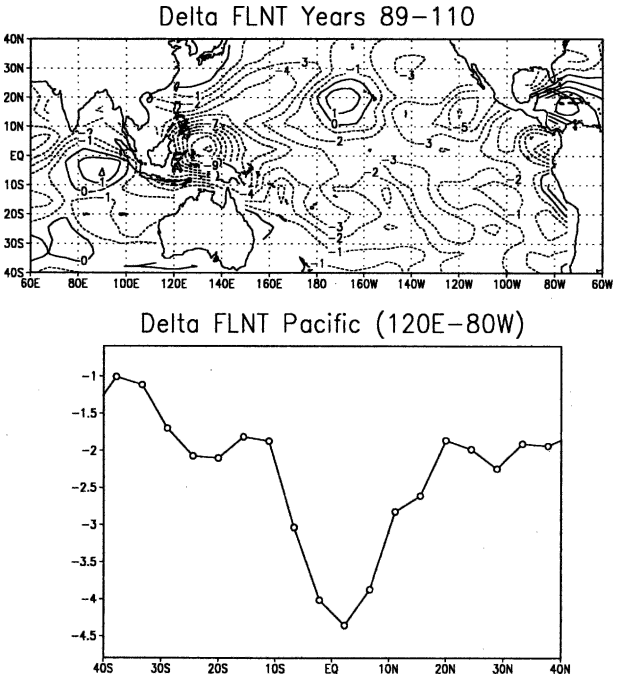

FIG. 4. Same as in Fig. 3 but for LW radiation loss at TOA (W m^{-2}).

SST is greater than the corresponding rate of infrared radiative loss by the surface. The SGE and anomalous LW pattern that occurs in our simulations can be explained by the anomalous high cloud coverage, which generally increases (decreases) during the simulation above the regions of maximum (minimum) warming, particularly in the deep Tropics (Fig. 5). A higher cloud deck causes a weaker longwave emission to space because the effective temperature of the cloud tops is reduced. We find that the near-equatorial Pacific warming and maximum SST increase east of Indonesia coincides with relatively large increases in high cloud cover (up to 0.03 fractional increase or +6%).

A key feature of the simulations is not just the spatial patterns by the end of the runs but the rate at which this quasi-equilibrium greenhouse response emerges. The enhanced warming of the near-equatorial region and especially the extreme western equatorial Pacific takes several decades to occur. Examining the temporal evolution of the changes in high clouds, SSTs, and precipitation, we see that the model's greenhouse "fingerprint" in the tropical Pacific is only clearly apparent during the last half of the simulations, when it emerges rapidly (Figs. 5–7). In particular, between years 23–66 and 67–110 the CO_2 fingerprint takes shape in terms of the near-equatorial enhanced warming, precipitation increase, and greater high-cloud amount. The last two variables are physically linked by atmospheric convection, which also increases quickly in the regions of rapid, maximum warming across the tropical Pacific. By focusing on the western equatorial Pacific, where the increases in SST, precipitation, and high cloudiness are largest, we see that the climatic response occurs rather abruptly (around year 80) between the time of doubling (year 70) and tripling (year 110) of initial CO_2 concentration (Fig. 8). The TOA LW anomaly starts out positive, but turns negative after about 10 yr and later sharply negative, dropping from around −6 to around −13 W m^{-2} after year 80. Similarly, there is a rapid increase in precipitation starting around year 80, when the rainfall rate jumps from around 3 to about 4 mm day^{-1} and remains at this much higher level thereafter. These rapid increases in implied greenhouse trapping and convection coincide with an abrupt rise in SST, which jumps from about 27° to more than 27.5°C around year 80. The large increase in precipitation and SST apparent early in the simulation—to around year 25—is dominated by the response of just one of the ensemble members, whose rainfall and temperatures subsequently drop back to near-modern values during the following two decades (not shown). We therefore attribute the early increase in precipitation and SST to natural variability, rather than to the crossing of a threshold temperature.

A potential explanation for this combination of rapid warming, precipitation increase, and greater high cloudiness during the latter half of the simulations is the known nonlinear relationship between SST and atmospheric convection in the Tropics. Observations from the tropical Indian and Pacific Oceans show an abrupt increase in convection where SSTs exceed about 27°C, when the moist enthalpy of the planetary boundary layer can provide enough convective instability to trigger organized deep convection (Graham and Barnett 1987; Betts and Ridgway 1989). FOAM1.5 reproduces this relationship in its modern control simulation (Fig. 9), such that both the model and observations indicate a frequency of large-scale rising motion of only 20% or less when SSTs are 26°C or lower but around a 90% frequency at surface temperatures of 29°C. The model's ability to reproduce this feature may be attributable to its cloud parameterization, which triggers deep convection when the convective available potential energy (CAPE) exceeds a threshold value. The cause of this abrupt increase in convection with warm SSTs has generally been attributed to the positive feedback of the SGE at high temperatures (Ramanathan and Collins 1991), a conclusion entirely consistent with the rapid decrease in TOA LW upon the transition to SSTs above 27°C in the simulations (Fig. 8).

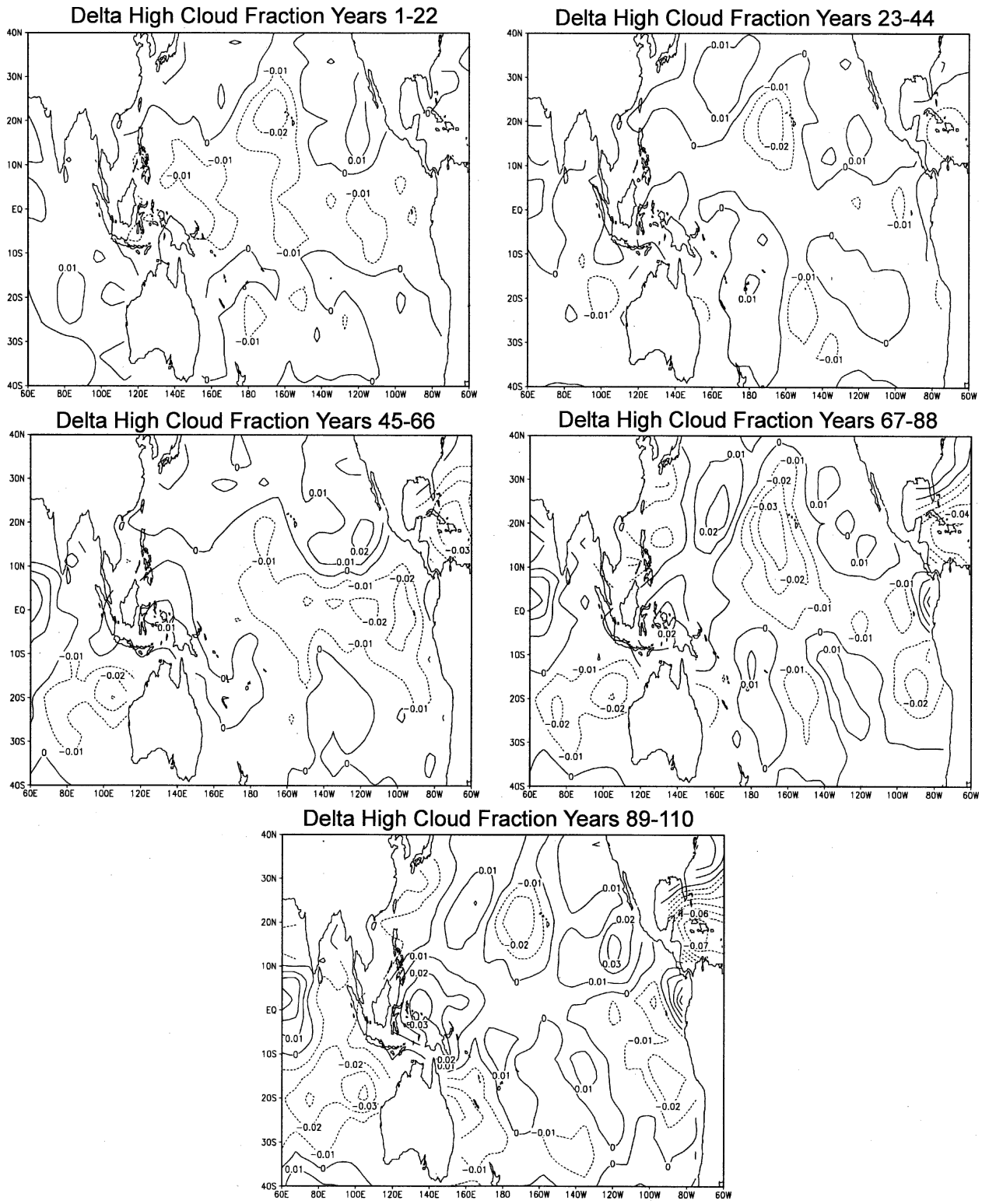

FIG. 5. Evolution of ensemble-mean anomalies of annual high cloud fraction during sequential 22-yr intervals of the transient CO_2 simulation.

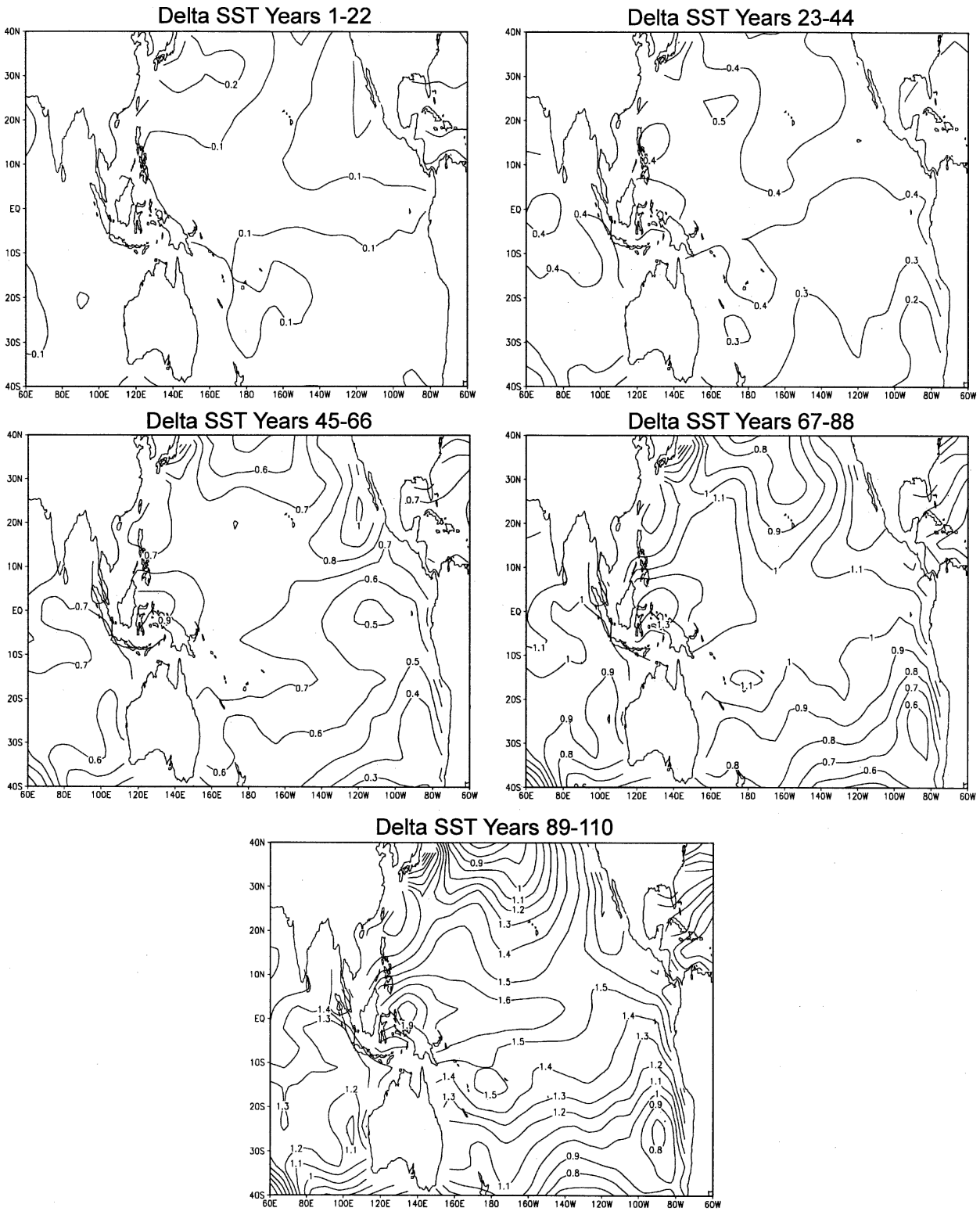

FIG. 6. Same as in Fig. 5 but for SSTs (K).

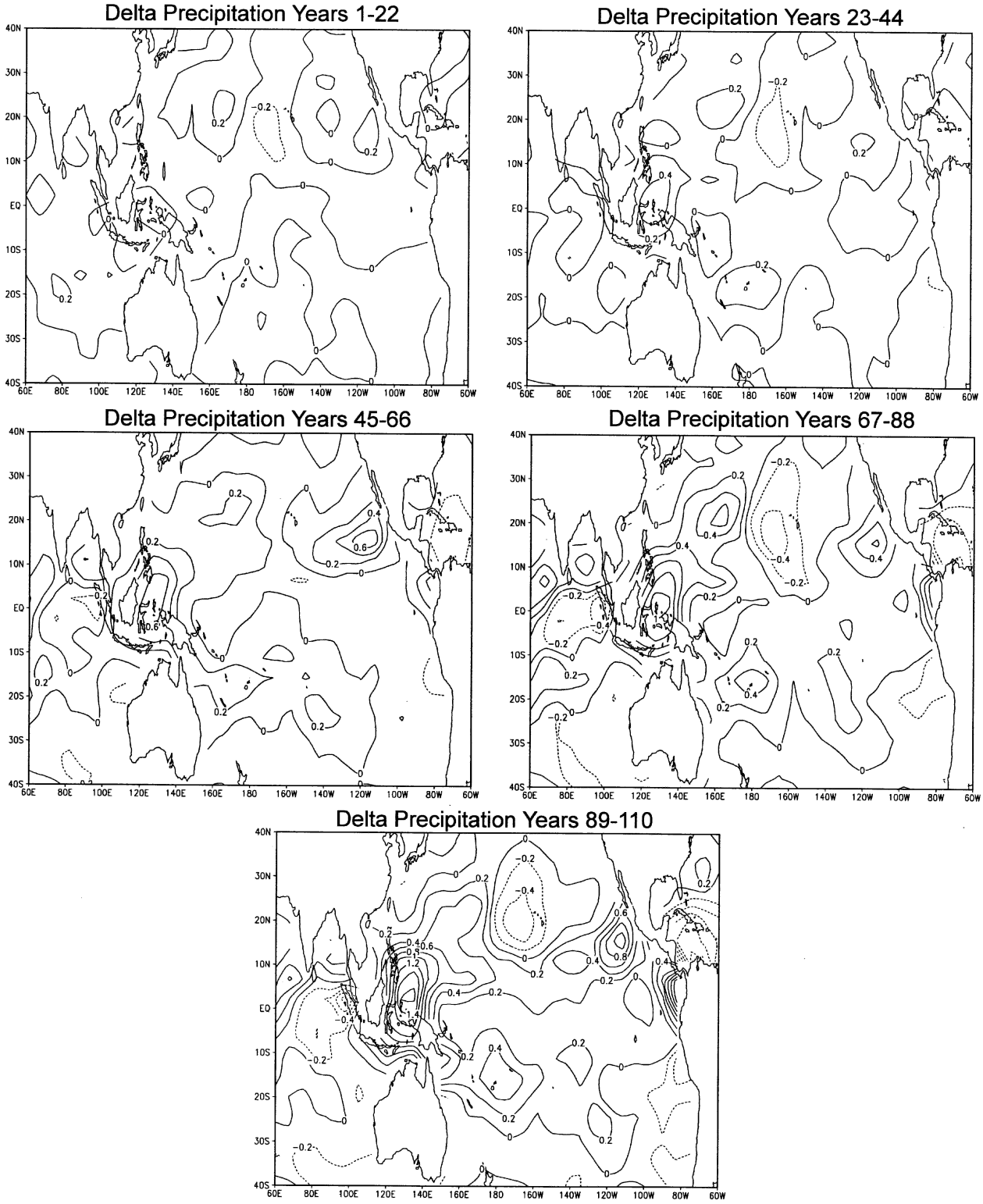

FIG. 7. Same as in Fig. 5 but for precipitation rate (mm day^{-1}).

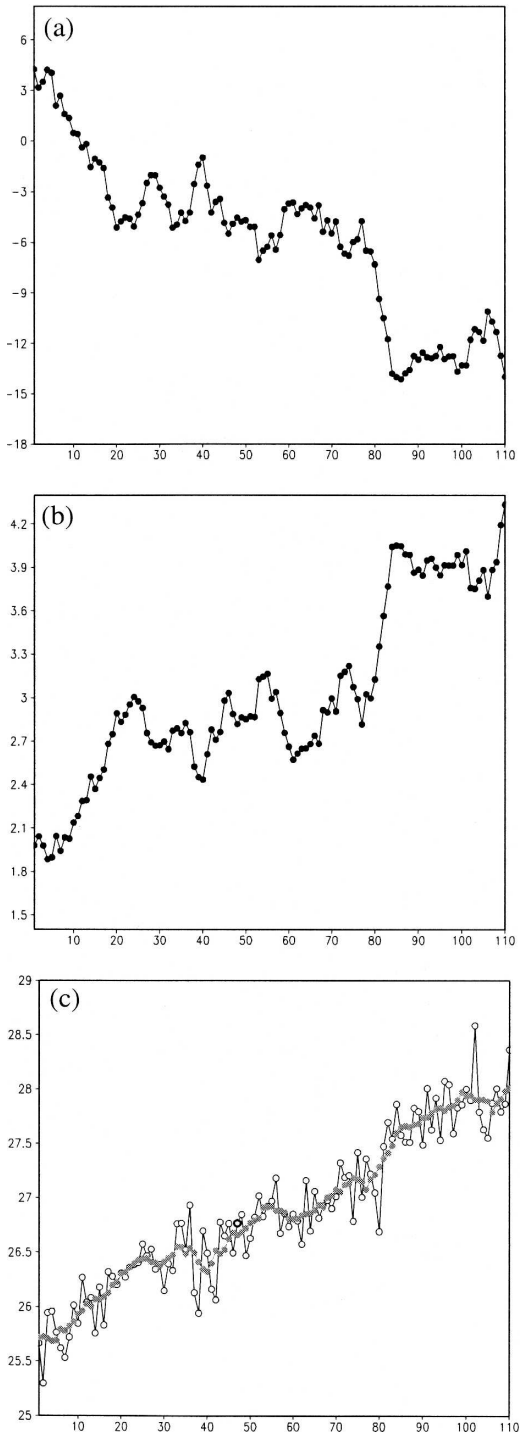

FIG. 8. 110-yr time series for the western equatorial Pacific grid point (2°N, 135°E) showing the largest warming trend. (a) Change in LW energy loss at TOA (W m^{-2}), (b) precipitation rate (mm day^{-1}), and (c) SST (°C). Curves with dark circles depict a 7-yr running mean, and open circles in bottom graph show individual years.

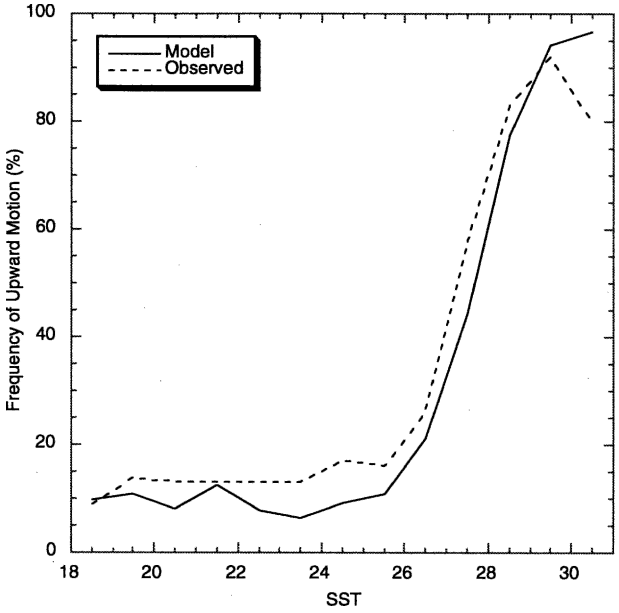

FIG. 9. Frequency of upward motion (%) at 500 hPa as a function of SST in the tropical Indo-Pacific region as observed (solid line) and simulated by FOAM1.5 (dashed) in its modern control run. Observed values are the NCEP–NCAR reanalysis data compiled by Bony et al. (1997).

Although this atmospheric process alone could account for the rapid deep tropical warming with transient greenhouse forcing, we also find another mechanism that contributes to the abrupt climatic response and represents a dynamical atmosphere–ocean feedback. The large and abrupt increase in near-equatorial convection over the western equatorial Pacific produces a secondary zonal circulation anomaly pattern consisting of rising atmospheric motion centered around 135°E and subsidence west of Indonesia, centered around 100°E (not shown). This circulation cell creates anomalous westerly winds within a few degrees of the equator and a substantial increase in westerly wind stress into the ocean over the western equatorial Pacific, extending to around 140°W (Fig. 10a). These westerly wind stress anomalies provide additional warming to the equatorial upper ocean through greater anomalous horizontal Ekman convergence (up to 6 W m^{-2} to the upper 40 m by the end of the simulation). Surprisingly, the upper ocean's vertical temperature advection along the equator actually decreases (causing a -4 W m^{-2} forcing), despite a reduction in upwelling caused by the westerly wind anomalies. This counterintuitive outcome results from the increased thermal stratification causing the remaining upwelling to have a more pronounced cooling effect on the upper ocean than the reduced upwelling has on thermal advection (Fig. 10b). The oceanic process causing the enhanced

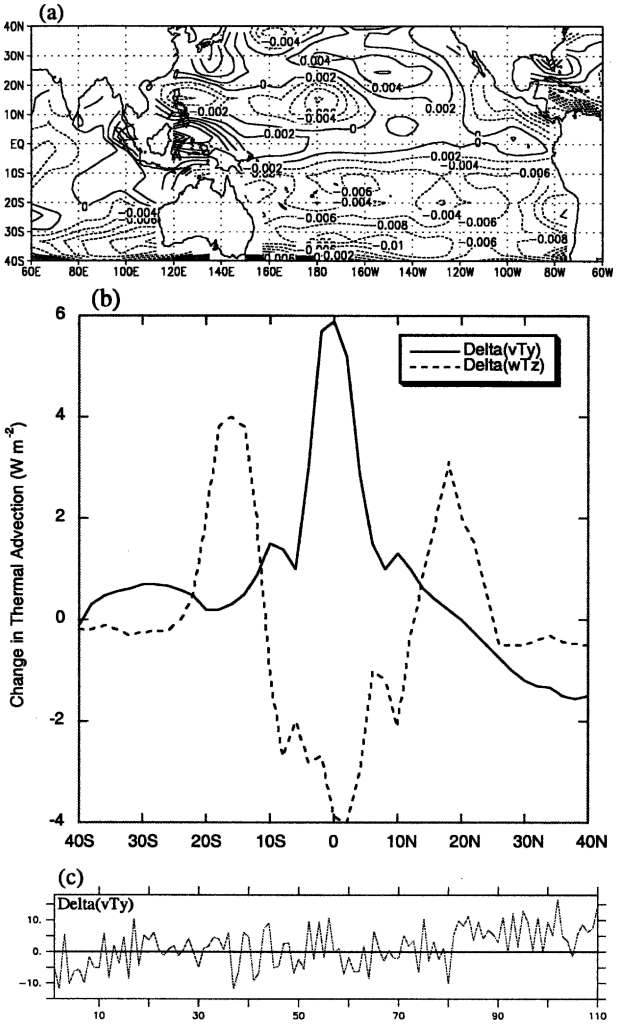

FIG. 10. (a) Same as in Fig. 4 (top) but for wind stress (N m^{-2}), (b) same as in Fig. 4 (bottom) but for meridional (vTy) and vertical (wTz) temperature advection (W m^{-2}) by Ekman transport in the upper 40 m of ocean, and (c) time series of anomalous meridional temperature advection (W m^{-2}) at 2°N, 135°E.

and rapid warming of the western equatorial Pacific is therefore Ekman convergence, which increases abruptly to a new and rather stable equilibrium after year 80, coinciding with the rapid SST increase at this time (Fig. 10c). Thus, the rapid warming east of Indonesia and extending across the near-equatorial Pacific is caused by both an atmospheric radiative feedback and a coupled atmosphere–ocean dynamical feedback.

b. Extratropical response

The behavior of the deep tropical Pacific Ocean has far-ranging impacts that affect the subtropical and midlatitude atmosphere. Many studies have found a linkage between tropical Pacific SST anomalies, such as those associated with ENSO, and atmospheric pressure teleconnections (Bjerknes 1969; Horel and Wallace 1981; Livezey et al. 1997). In particular, the strength of the wintertime Aleutian low is known to be highly sensitive to the tropical ocean heating, such that this semipermanent cyclone tends to be unusually strong during warm Pacific events (El Niños; van Loon and Madden 1981; Livezey et al. 1997). FOAM1.5 captures this teleconnective forcing in the greenhouse simulations, both in terms of the gradual deepening of the Aleutian low and the rapidity of the strengthening after the abrupt warming and convection increase in the near-equatorial Pacific (Fig. 11). A possible explanation for this relationship is Rossby wave propagation, which requires tropical vortex stretching due to enhanced convection (Hoskins and Karoly 1981). The rapid drop and sustained negative anomalies in upper-tropospheric heights over the North Pacific during the ninth decade appear to be caused by the rapid and sustained deep tropical changes described above, even though there is

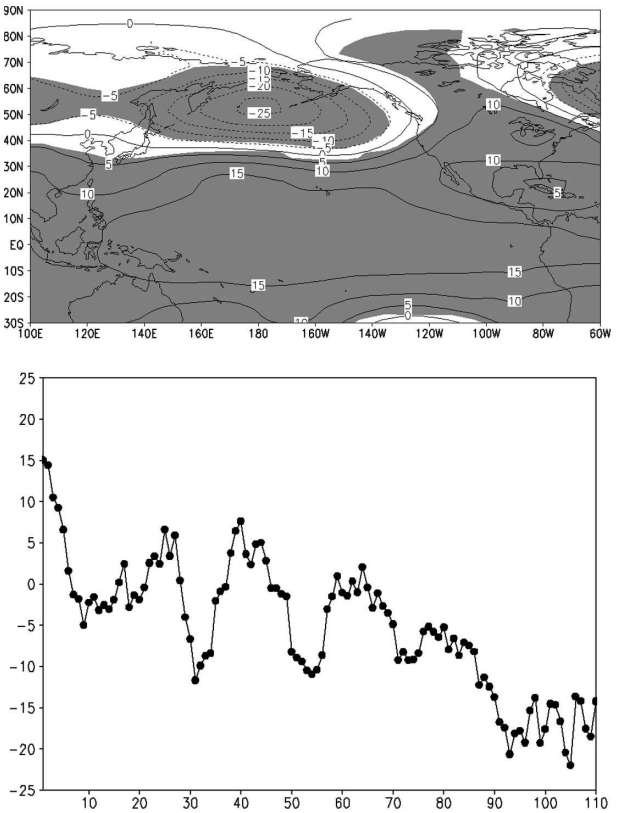

FIG. 11. (top) Change from control in ensemble-mean annual upper-air (250 hPa) geopotential height (m) during the final two decades of the transient CO_2 simulation (with global-mean change subtracted and 95% confidence regions shaded), and (bottom) time series of this difference averaged over the North Pacific (40°–60°N, 160°E–140°W).

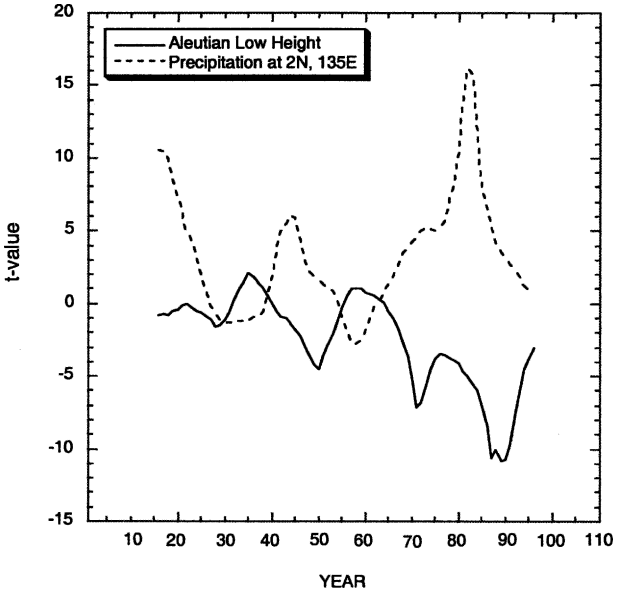

FIG. 12. Values of a scanning *t* test for the difference between subsample 15-yr means of upper-air Aleutian low height taken from Fig. 11b (solid) and western equatorial Pacific precipitation rate from Fig. 8b (dashed).

a time delay of a few years between the most rapid tropical response (years 79–84) and the most rapid upper-air height falls (beginning in year 86). This delay in the ensemble-mean response, which is caused by the behavior of one of the three ensemble members, may result from the strong internal variability of the Aleutian low. The large natural variability of this feature is known to complicate efforts to isolate its response to tropical SST forcing (Trenberth et al. 1998).

To quantify the timing and magnitude of rapid changes in the Aleutian low and tropical convection, we applied a scanning (or sequential) *t* test. This statistical tool, an extension of the classical Student's *t* test to determine the significance of the difference between two subsample means, has been used in other studies to detect abrupt climate change (Jiang and You 1996; Jiang et al. 2002). Using a subsample interval of 15 yr on either side of a given point in the 110-yr time series, we scan the evolution of the area-averaged Aleutian low heights shown in Fig. 11b and the western equatorial precipitation shown in Fig. 8b. The results of the scanning *t* test (Fig. 12) indicate that the most pronounced changes in these quantities occur within the ninth decade of the run. Tropical convection shows a sharp increase centered at years 82–83, while the Aleutian low exhibits its strongest deepening over a slightly broader transition period centered at years 87–90. The large *t* values at these times depict not only the large rates of change occurring during these transitions but also the relative consistency of the quantities following the transition. For tropical rainfall this jump represents a change from less than 3 mm day^{-1} to a quasi-equilibrium value of almost 4 mm day^{-1} (Fig. 8b), and for the Aleutian low a deepening from less than −10 m anomalies to departures that vary around −15 to −20 m (Fig. 11b). This statistical test thus helps to isolate transitions to quasi-equilibrium states compared with temporary fluctuations, such as the Aleutian low height falls during years 25–30 and 45–50 that do not persist.

The atmospheric changes over the North Pacific represent an example of abrupt tropical change causing a corresponding response in the extratropics, both within the subpolar region (where the Aleutian low deepens) and over the subtropics–midlatitudes, where the deepened Aleutian low increases the meridional pressure gradient aloft and thus causes a stronger Pacific jet stream from around 30°–50°N (up to 1.6 m s^{-1} or +5%). The enhanced deep tropical heating also produces much greater poleward energy transport emanating from the western equatorial Pacific that promotes extratropical atmospheric heating. When the model was run to equilibrium under 2 × CO_2 forcing, the vertically integrated atmospheric energy divergence increased by a maximum of over 20% at 2°N (zonally averaged) and by 15% across the entire near-equatorial region from 5°S–5°N, resulting in a gain of poleward energy flux convergence in mid–high latitudes (45°–90°) of nearly 5% annually. These changes are consistent with the large observed increases in poleward atmospheric energy transport emanating from the anomalously warm deep tropical Pacific during El Niños (Trenberth et al. 2002a,b).

The importance of tropical heating for the remote response of the Aleutian low is underscored by two supplemental transient CO_2 experiments, one of which suppressed ocean wind stress changes globally and thus the positive Ekman convergence feedback in the western equatorial Pacific (PCNWC), while the other suppressed all SST increases over the Tropics (30°N–30°S) during the simulations (PC1). Both of these supplemental experiments were driven by the same 110-yr transient CO_2 increase and utilize the partial coupling (PC) "modeling surgery" techniques described in detail by Wu and Liu (2003). Compared with the time evolution of deep tropical heating in the standard experiments, the elimination of the wind stress feedback causes much less interannual variability of ocean heating east of Indonesia and a smaller overall warming of about 0.3 K (Fig. 13, cf. Fig. 8), along with a shift in the maximum tropical Pacific warming from the equator to 5°–10°N (not shown). SSTs of 27.5°C in the western equatorial Pacific do not emerge until the final 10 yr of the simu-

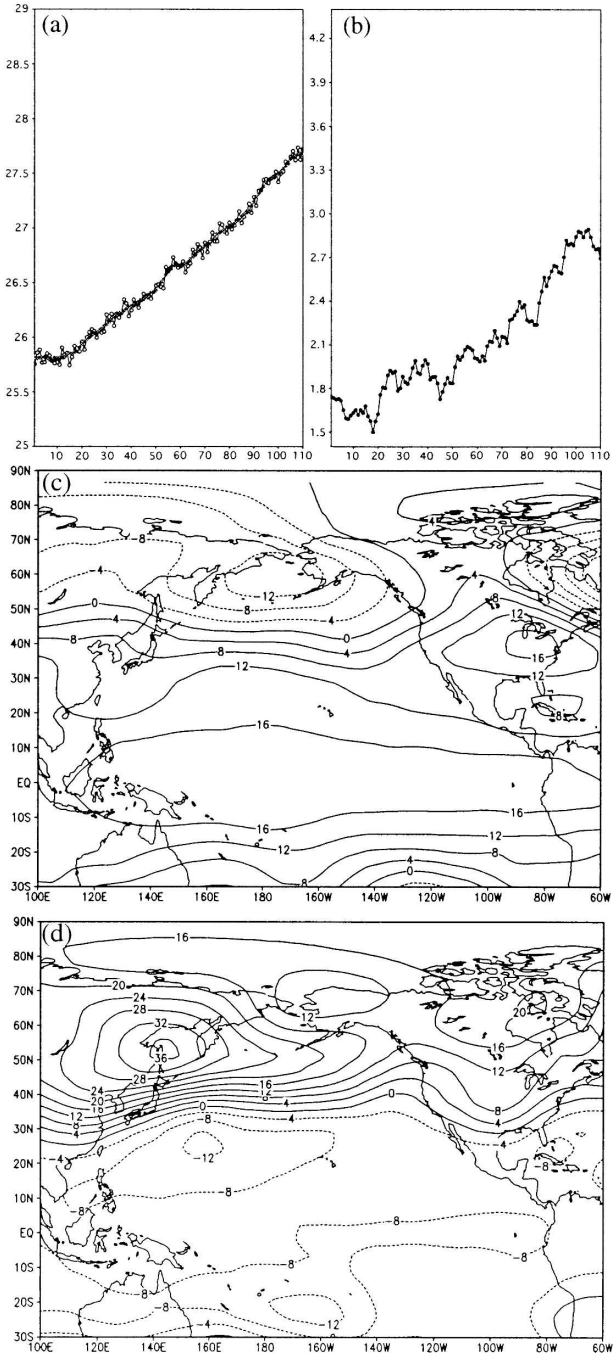

FIG. 13. (a), (b) Same as in Figs. 8c,b but for a simulation with no change in ocean wind stress (PCNWC), (c) same as in Fig. 11 (top) but for PCNWC, and (d) same as in Fig. 11 (top) but for a simulation with no tropical SST increase (PC1).

lation, compared with the final 30 yr if this added oceanic heating mechanism is allowed. Similarly, the precipitation increase in PCNWC is much smaller and less abrupt, with the precipitation rate in the western equatorial Pacific never exceeding 3 mm day^{-1}, compared with over 4 mm day^{-1} by the end of the standard simulations (Figs. 13a,b). Consistent with this muted tropical response, the Aleutian low deepens by only half as much in PCNWC by the last two decades of the simulations, and the Pacific jet aloft is correspondingly much less strengthened (Fig. 13c). As an extreme example of tropical forcing on extratropical circulation, the run with no tropical ocean warming (PC1) not only eliminates strengthening of the Aleutian low but instead generates substantial height rises over the North Pacific and eastern Asia (Fig. 13d). Thus, in this model at least, tropical forcing appears to be the primary driver of the extratropical response in atmospheric circulation over the North Pacific.

4. Discussion

We propose that strong tropical forcing may be an inherent property of the climate system through the existence of a critical SST threshold for large-scale convection, which may be crossed in a warming scenario as very warm water in the western tropical Pacific and eastern Indian Ocean migrates eastward. This kind of behavior occurs during modern El Niño events, when major convective anomalies emerge over the central equatorial Pacific, but an important difference between this observed feature and what we propose for a warmer mean climate is that the impact of the former pattern is somewhat tempered by offsetting cooling within the west Pacific warm pool, whereas the warm pool expands in the case of climatic warming. In the model used here the simulated Indo-Pacific warm pool in the modern climate is located too far to the west (Fig. 1), due to a common bias in coupled models that the equatorial cold tongue extends too far westward. This bias undoubtedly affects where the rapid SST rise is simulated, but the basic process by which the abrupt warming occurs should still apply to an altered climate scenario. For example, a similar rapid equatorial warming arises late in the CSM1's transient CO_2 simulation but is shifted eastward (170°E), because the cold tongue bias is less pronounced in that model. One caveat, however, is that because FOAM1.5's equatorial cold tongue extends too far west, the model's dynamical oceanic response to westerly wind anomalies (such as the kind depicted in Fig. 10) may be an unrealistic warming of the western equatorial Pacific, due to the Ekman heat convergence described in section 3a. In reality, westerly wind bursts during the Madden–Julian oscillation (MJO) events cause SST decreases in this region (Yu and Rienecker 1998; McPhaden 1999), although sometimes this cooling may stem more from occasional wintertime outflow of cold Eurasian air

masses over the western Pacific than from the intratropical, time-mean wind changes occurring in our transient CO_2 simulation.

The results presented here are probably model dependent and especially sensitive to how clouds and convection are parameterized. The essential uncertainties are how much high, heat-trapping clouds increase under an externally forced warming, whether this increase is offset by decreases in adjacent cloudiness (i.e., the Iris mechanism; Lindzen et al. 2001), and what is the associated radiative competition between less incoming solar radiation and less outgoing terrestrial radiation due to greater cirrus cloudiness. Ramanathan and Collins (1991) proposed a strong negative cloud feedback resulting from tropical heating, as the increase in cirrus clouds would reduce incoming solar radiation more than it would enhance the trapping of longwave radiation. There is evidence that the atmospheric component of FOAM1.5 (CCM3) may overestimate the positive feedback from cloud changes induced by interannual SST variations in the eastern tropical Pacific, by exaggerating the anomalous positive longwave cloud radiative forcing (CRF) relative to the negative shortwave CRF anomaly (Sun et al. 2003). Using the same GCM, however, Meehl et al. (2000) found that the net change in cloud radiative forcing over both the eastern and western equatorial Pacific was negative when the model is subjected to a $2 \times CO_2$ radiative perturbation (this result applies to the CCM3 version that uses the same diagnostic cloud liquid water parameterization used in FOAM1.5). The latter result is more pertinent for our greenhouse forcing experiment and suggests that the rapid tropical warming generated by FOAM1.5 may not be an artifact of the model's cloud parameterization. However, we note that even though Meehl et al. (2000) reported a negative change in CRF, their model may still underestimate the actual cloud feedback in this region.

Another issue regarding the relevance of our results concerns the model's positive dynamical ocean feedback, which enhances the tropical SST increase and the extratropical response (Fig. 13). Some studies, such as Clement et al. (1996) and Sun and Liu (1996) suggest that dynamical atmosphere–ocean coupling between the relatively warm western equatorial Pacific and the cooler eastern equatorial Pacific would help to moderate heating of the warm pool through an increase in the strength of the Walker circulation. In this scenario, a heating anomaly such as increased CO_2 would strengthen the climatological mean easterly winds over the equator and thus cause greater advection of relatively cool ocean water from the eastern basin to the west. These earlier studies, however, were conducted with simpler models that did not include the range of atmospheric feedbacks that occur in fully coupled atmosphere–ocean GCMs, such as FOAM1.5. Many subsequent simulations using these more sophisticated climate models have shown a reduction in equatorial easterly winds similar to the pattern generated by FOAM1.5 (Fig. 10; Knutson and Manabe 1998; Yu and Boer 2002; Vavrus and Liu 2002).

Dynamical changes such as these could affect or be associated with ENSO and thus influence the simulated warming in the western equatorial Pacific. Sun et al. (2003), for example, suggests that an increase of the warm pool SST should generate stronger El Niños, which would cause greater tropical oceanic heat export and damp the temperature rise in the western equatorial Pacific. This type of response does not occur in our greenhouse gas simulation. The model produces a reasonable ENSO in the control run, with peak variance in the 2–7-yr band but an amplitude about 20% weaker than observed, possibly due to a thermocline that is too diffusive (Liu et al. 2000). When FOAM1.5 is run to equilibrium under constant $2 \times CO_2$ radiative forcing, the amplitude of ENSO weakens by approximately 10% compared with the model's modern control run. Thus, the large warming in the western equatorial Pacific is not mitigated by stronger El Niños.

The rapid low-latitude warming and associated remote extratropical responses depicted here provide an example of how the Tropics could initiate or hasten abrupt, large-scale climate change. Recent paleoclimatic evidence indicates that temperature changes in the Tropics have often preceded climate changes in the extratropics and that these tropical variations have sometimes been abrupt. Cane and Molnar (2001) and Molnar and Cane (2002) proposed that the extreme extratropical warmth of the early–middle Pliocene epoch around 3–5 million years ago was caused primarily by vigorous poleward atmospheric heat transport stemming from very warm tropical Pacific SSTs ("a virtually permanent El Niño–like state"), and the subsequent high-latitude cooling and formation of ice sheets was initiated by a large reduction in poleward heat transport due to the initiation of a pronounced Walker circulation. During the more recent geological record, glaciers in the Andes and coral reefs near Barbados show that tropical warming commenced prior to the most recent deglaciation in the Northern Hemisphere (Guilderson et al. 2001; Seltzer et al. 2002), while the near synchroneity of rapid tropical Atlantic and Greenland warming over this time interval is attributed to a sudden southward shift in the ITCZ (Lea et al. 2003). Within the Indo-Pacific warm pool, in the region showing the abrupt warming in our future simulation, field

evidence indicates that similar large, rapid SST increases occurred during recent deglaciations and that these tropical warmings preceded melting of boreal ice sheets, suggestive of a low-latitude forcing mechanism (Lea et al. 2000; Visser et al. 2003). Remarkably, these past western equatorial Pacific warmings even display the same rapid rise around 27°C simulated by FOAM1.5, prompting de Deckker et al. (2002) to propose that this region crosses convective thresholds, which provide a large positive feedback affecting climate worldwide and that initiated modern patterns of monsoonal rainfall over Southeast Asia following deglaciation around 12–11 ka BP.

Modeling support also exists for paleoclimatic tropical Pacific triggers. Clement et al. (2001) suggested that the Younger Dryas cooling originated from prolonged La Niña conditions. Yin and Battisti (2001) showed that even small (1 K) changes in mean tropical SSTs at the Last Glacial Maximum (LGM) caused changes in convection large enough to affect the general circulation on a global scale. Furthermore, the LGM simulation by Shin et al. (2003) found that the maximum response (cooling) in the deep tropical Pacific occurred in the western equatorial region, in the same area shown to be especially sensitive to positive radiative forcing in our simulation.

5. Conclusions

A coupled, global atmosphere–ocean GCM forced with transiently increasing CO_2 simulates a highly nonuniform warming pattern across the tropical and midlatitude Pacific Ocean. Maximum SST increases occur in the near-equatorial regions, especially in the far western basin, where the warming peaks just east of Indonesia. The evolution of enhanced deep tropical warming is not monotonic, but instead is delayed for several decades and emerges abruptly around year 80, between the time of CO_2 doubling and tripling. The critical ingredient for this rapid warming appears to be the existence of a critical SST threshold for vigorous convection (around 27°C). As imposed greenhouse forcing gradually warms the ocean, the eastward expansion of the Indo-Pacific warm pool causes regions of the equatorial Pacific to warm beyond this temperature threshold and thus generate much greater convection. The enhanced convection triggers two related positive feedbacks, one of which is an atmospheric process and the other is oceanic but involves atmosphere–ocean coupling. The atmospheric feedback consists of enhanced atmospheric convection leading to a stronger super–greenhouse effect, due to increased high cloudiness emitting less longwave radiation to space. The oceanic feedback is driven by greater Ekman heat convergence, due to the emergence of a westerly surface wind anomaly that results from the enhanced atmospheric convection. Of these two feedbacks, the atmospheric response is the critical one, because the enhanced Ekman convergence in the ocean only ensues as a result of the westerly wind anomaly that is first created by the anomalous atmospheric convection. Without the reinforcing oceanic feedback, however, the equatorial climatic response is weaker, less abrupt, and generates a weaker extratropical teleconnection.

The relatively strong and abrupt deep tropical warming corresponds with a remote response in the extratropics. The timing and type of changes in the Aleutian low (deepening) and Pacific jet stream (strengthening) suggest a forcing of tropical origin, based on known teleconnections in the modern climate. Because rapid changes in these extratropical features follow the abrupt warming and enhanced convection in the deep Tropics, this study illustrates a possible manner by which rapid tropical climate changes could trigger abrupt changes in mid- and high latitudes. Recent studies have provided evidence for such tropical initiation in the past, but they have lacked a clear physical explanation for how relatively small but rapid changes in tropical temperatures could generate large-scale climate changes. While the simulated remote changes described here did not produce correspondingly abrupt changes in temperature or precipitation over boreal landmasses, the model provides a plausible linkage to explain how a tropical trigger might operate. Future studies with higher-resolution models and different cloud parameterizations may yield further insight and offer a better evaluation of the results shown here.

Acknowledgments. This work was supported by NSF Grant ATM 0002937 and DOE Grant DE-FG02-01ER63249. We appreciate the assistance from Yafang Zhong in producing the figures and from Lixin Wu for providing the partial coupling code.

REFERENCES

Betts, A. K., and W. Ridgway, 1989: Climatic equilibrium of the atmospheric convective boundary layer over a tropical ocean. *J. Atmos. Sci.,* **46,** 2621–2641.

Bjerknes, J., 1969: Atmospheric teleconnections from the equatorial Pacific. *Mon. Wea. Rev.,* **97,** 163–172.

Bony, S., K.-M. Lau, and Y. C. Sud, 1997: Sea surface temperature and large-scale circulation influences on tropical greenhouse effect and cloud radiative forcing. *J. Climate,* **10,** 2055–2077.

Boville, B. A., and P. R. Gent, 1998: The NCAR Climate System Model, version one. *J. Climate,* **11,** 1115–1130.

Branstator, G., 1985: Analysis of general circulation model sea

surface temperature anomaly simulations using a linear model. Part I: Forced solutions. *J. Atmos. Sci.,* **42,** 2225–2241.

Cai, W., and P. H. Whetton, 2000: Evidence for a time-varying pattern of greenhouse warming in the Pacific Ocean. *Geophys. Res. Lett.,* **27,** 2577–2580.

Cane, M. A., and P. Molnar, 2001: Closing of the Indonesian seaway as a precursor to east African aridification around 3-4 million years ago. *Nature,* **411,** 157–162.

Chase, T. N., R. A. Pielke Sr., T. G. F. Kittel, R. R. Nemani, and S. W. Running, 2000: Simulated impacts of historical land cover changes on global climate in northern winter. *Climate Dyn.,* **16,** 93–105.

Clement, A. C., R. Seager, M. A. Cane, and S. E. Zebiak, 1996: An ocean dynamical thermostat. *J. Climate,* **9,** 2190–2196.

——, M. C. Cane, and R. Seager, 2001: An orbitally driven tropical source for abrupt climate change. *J. Climate,* **14,** 2369–2375.

De Deckker, P., N. J. Tapper, and S. vander Kaars, 2002: The status of the Indo-Pacific warm pool and adjacent land at the Last Glacial Maximum. *Global Planet. Change,* **35,** 25–35.

Delire, C., P. Behling, M. Coe, J. A. Foley, R. Jacob, J. Kutzbach, Z. Liu, and S. Vavrus, 2001: Simulated response of the atmosphere-ocean system to deforestation in the Indonesian Archipelago. *Geophys. Res. Lett.,* **28,** 2081–2084.

Graham, N. E., and T. P. Barnett, 1987: Sea surface temperature, surface wind divergence, and convection over tropical oceans. *Science,* **238,** 657–659.

Guilderson, T. P., R. G. Fairbanks, and J. L. Rubenstone, 2001: Tropical Atlantic coral oxygen isotopes: Glacial-interglacial sea surface temperatures and climate change. *Mar. Geol.,* **172,** 75–89.

Harrison, S., J. Kutzbach, Z. Liu, P. J. Bartlein, B. Otto-Bliesner, D. Muhs, I. C. Prentice, and R. S. Thompson, 2003: Mid-Holocene climates of the Americas: A dynamical response to changed seasonality. *Climate Dyn.,* **20,** 663–688.

Hoerling, M. P., J. W. Hurrell, and T. Xu, 2001: Tropical origins for recent North Atlantic climate change. *Science,* **292,** 90–92.

Holland, M. M., and C. M. Bitz, 2003: Polar amplification of climate change in the coupled model intercomparison project. *Climate Dyn.,* **21,** 221–232.

Horel, J. D., and J. M. Wallace, 1981: Planetary-scale atmospheric phenomena associated with the Southern Oscillation. *Mon. Wea. Rev.,* **109,** 813–829.

Hoskins, B. J., and D. J. Karoly, 1981: The steady linear response of a spherical atmosphere to thermal and orographic forcing. *J. Atmos. Sci.,* **38,** 1179–1196.

Houghton, J. T., Y. Ding, D. J. Griggs, M. Noguer, P. J. van der Linden, X. Dai, K. Maskell, and C. A. Johnson, Eds., 2001: *Climate Change 2001: The Scientific Basis*. Cambridge University Press, 944 pp.

Jacob, R., 1997: Low frequency variability in a simulated atmosphere-ocean system. Ph.D. thesis, University of Wisconsin—Madison, 159 pp.

Jiang, J., and X. T. You, 1996: Where and when did an abrupt climate change occur in China during the last 43 years? *Theor. Appl. Climatol.,* **55,** 33–39.

——, R. Mendelssohn, F. Schwing, and K. Fraedrich, 2002: Coherency detection of multiscale abrupt changes in historic Nile flood levels. *Geophys. Res. Lett.,* **29,** 1271, doi:10.1029/2002GL014826.

Kalnay, E., and Coauthors, 1996: The NCEP/NCAR 40-Year Reanalysis Project. *Bull. Amer. Meteor. Soc*., **77,** 437–471.

Kiehl, J. T., J. J. Hack, G. B. Bonan, B. A. Boville, D. L. Williamson, and P. J. Rasch, 1998: The National Center for Atmospheric Research Community Climate Model: CCM3. *J. Climate,* **11,** 1131–1149.

Knutson, T. R., and S. Manabe, 1995: Time-mean response over the tropical Pacific to increased CO_2 in a coupled ocean-atmosphere model. *J. Climate,* **8,** 2181–2199.

——, and ——, 1998: Model assessment of decadal variability and trends in the tropical Pacific Ocean. *J. Climate,* **11,** 2273–2296.

Lea, D. W., D. K. Pak, and H. J. Spero, 2000: Climate impact of late Quaternary equatorial Pacific sea surface temperature variations. *Science,* **289,** 1719–1724.

——, ——, L. C. Peterson, and K. A. Hughen, 2003: Synchroneity of tropical and high-latitude Atlantic temperatures over the last glacial termination. *Science,* **301,** 1361–1364.

Levitus, S., 1982: *Climatological Atlas of the World Ocean*. NOAA Prof. Paper 13, 173 pp. and 17 microfiche.

Lindzen, R. S., M. D. Chou, and A. Y. Hou, 2001: Does the Earth have an adaptive infrared iris? *Bull. Amer. Meteor. Soc.,* **82,** 417–432.

Liu, Z., J. Kutzbach, and L. Wu, 2000: Modeling climate shift of El Niño variability in the Holocene. *Geophys. Res. Lett.,* **27,** 2265–2268.

——, B. Otto-Bliesner, J. Kutzbach, L. Li, and C. Shields, 2003: Coupled climate simulation of the evolution of global monsoons in the Holocene. *J. Climate,* **16,** 2472–2490.

——, S. Vavrus, and F. He, 2005: Rethinking tropical ocean response to global warming: The enhanced equatorial warming. *J. Climate,* **18,** 4684–4700.

Livezey, R. E., M. Masutani, A. Leetmaa, H. Rui, M. Ji, and A. Kumar, 1997: Teleconnective response of the Pacific–North American region atmosphere to large central equatorial Pacific SST anomalies. *J. Climate,* **10,** 1787–1820.

McPhaden, M. J., 1999: Genesis and evolution of the 1997-98 El Niño. *Science,* **283,** 950–954.

Meehl, G. A., and W. M. Washington, 1986: Tropical response to increased CO_2 in a GCM with a simple mixed layer ocean: Similarities to an observed Pacific warm event. *Mon. Wea. Rev.,* **114,** 667–674.

——, W. D. Collins, B. Boville, J. T. Kiehl, T. M. L. Wigley, and J. M. Arblaster, 2000: Response of the NCAR Climate System Model to increased CO_2 and the role of physical processes. *J. Climate,* **13,** 1879–1898.

Molnar, P., and M. A. Cane, 2002: El Niño's tropical climate and teleconnections as a blueprint for pre-Ice Age climates. *Paleoceanography*, **17,** 1021, doi:10.1029/2001PA000663.

Murtugudde, R., J. Beauchamp, C. R. McClain, and A. J. Busalacchi, 2002: Effects of penetrative radiation on the upper tropical ocean circulation. *J. Climate,* **15,** 470–486.

Neale, R., and J. Slingo, 2003: The Maritime Continent and its role in the global climate: A GCM study. *J. Climate,* **16,** 834–847.

Notaro, M., Z. Liu, R. Gallimore, S. J. Vavrus, J. E. Kutzbach, I. C. Prentice, and R. L. Jacob, 2005: Simulated and observed preindustrial to modern vegetation and climate changes. *J. Climate,* **18,** 3650–3671.

Poulsen, C. A., 2003: Absence of runaway ice-albedo feedback in the Neoproterozoic. *Geology,* **31,** 115–118.

Ramanathan, V., and W. Collins, 1991: Thermodynamic regulation of ocean warming by cirrus clouds deduced from observations of the 1987 El Niño. *Nature,* **351,** 27–32.

Robertson, A. W., C. R. Mechoso, and Y. J. Kim, 2000: The influence of Atlantic sea surface temperature anomalies on the North Atlantic Oscillation. *J. Climate,* **13,** 122–138.

Seltzer, G. O., D. T. Rodbell, P. A. Baker, S. C. Fritz, P. M. Tapia, H. D. Rowe, and R. B. Dunbar, 2002: Early warming of tropical South America at the last glacial-interglacial transition. *Science,* **296,** 1685–1686.

Shin, S., Z. Liu, B. Otto-Bliesner, E. C. Brady, J. E. Kutzbach, and S. Harrison, 2003: A simulation of the Last Glacial Maximum climate using the NCAR-CCSM. *Climate Dyn.,* **20,** 127–151.

Sun, D. Z., and Z. Liu, 1996: Dynamic ocean-atmosphere coupling: A thermostat for the tropics. *Science,* **272,** 1148–1150.

——, J. Fasullo, T. Zhang, and A. Roubicek, 2003: On the radiative and dynamical feedbacks over the equatorial Pacific cold tongue. *J. Climate,* **16,** 2425–2432.

Terray, L., and C. Cassou, 2002: Tropical Atlantic sea surface temperature forcing of quasi-decadal climate variability over the North Atlantic–European region. *J. Climate,* **15,** 3170–3187.

Trenberth, K. E., G. W. Branstator, D. Karoly, A. Kumar, N. C. Lau, and C. Ropelewski, 1998: Progress during TOGA in understanding and modeling global teleconnections associated with tropical sea surface temperatures. *J. Geophys. Res.,* **103** (C7), 14 291–14 324.

——, J. M. Caron, D. P. Stepaniak, and S. Worley, 2002a: Evolution of El Niño–Southern Oscillation and global atmospheric surface temperatures. *J. Geophys. Res*., **107,** 4065, doi: 10.1029/2000JD000298.

——, D. P. Stepaniak, and J. M. Caron, 2002b: Interannual variations in the atmospheric heat budget. *J. Geophys. Res*., **107,** 4066, doi:10.1029/2000JD000297.

van Loon, H., and R. A. Madden, 1981: The Southern Oscillation. Part I: Global associations with pressure and temperature in northern winter. *Mon. Wea. Rev.,* **109,** 1150–1162.

Vavrus, S., and Z. Liu, 2002: Toward understanding the response of the tropical atmosphere-ocean system to increased CO_2 using equilibrium asynchronous coupling. *Climate Dyn.,* **19,** 355–369.

Visser, K., R. Thunell, and L. Stott, 2003: Magnitude and timing of temperature change in the Indo-Pacific warm pool during deglaciation. *Nature,* **421,** 152–155.

Wu, L., and Z. Liu, 2003: Decadal variability in the North Pacific: The eastern North Pacific mode. *J. Climate,* **16,** 3111–3131.

——, ——, R. Gallimore, R. Jacob, D. Lee, and Y. Zhong, 2003: A coupled modeling study of Pacific decadal variability: The tropical Pacific mode and the North Pacific mode. *J. Climate,* **16,** 1101–1129.

Yin, J. H., and D. S. Battisti, 2001: The importance of tropical sea surface temperature patterns in simulations of Last Glacial Maximum climate. *J. Climate,* **14,** 565–581.

Yu, B., and G. J. Boer, 2002: The roles of radiation and dynamical processes in the El Niño–like response to global warming. *Climate Dyn.,* **19,** 539–553.

Yu, L., and M. M. Rienecker, 1998: Evidence of an extratropical atmosphere influence during the onset of the 1997–98 El Niño. *Geophys. Res. Lett.,* **25,** 3537–3540.